

Chapter 14

Grid Frequency Mitigation Using SMES of Optimum Power and Energy Storage Capacity

M. R. I. Sheikh and J. Tamura

Abstract Considering the viewpoint of cost-effectiveness, a computational method to determine the SMES power rating needed to minimize the grid frequency fluctuation is analyzed in this chapter. Moreover, the required minimum energy storage capacity of SMES unit is determined. Finally, simulation results using pulse width modulation (PWM) based voltage source converter (VSC) and two-quadrant DC–DC chopper-controlled SMES system are presented. It is seen that the proposed SMES system with required minimum energy storage capacity can significantly decrease the voltage and output power fluctuations of wind farm, which consequently mitigate the grid frequency fluctuation.

14.1 Introduction

14.1.1 Renewable Energy

We are now at a crucial cross board of our global energy scenario. Energy has been the life hood of the continual progress of human civilization. Since the industrial revolution of the two centuries ago, global energy consumption has increased by leaps and bounds to improve our living standards, particularly in the industrialized nations of the world.

M. R. I. Sheikh (✉)

EEE Department, Rajshahi University of Engineering & Technology,
Rajshahi 6204, Bangladesh
e-mail: ris_ruet@yahoo.com

J. Tamura

EEE Department, Kitami Institute of Technology, 165 Koen-cho,
Kitami 090-8507, Japan

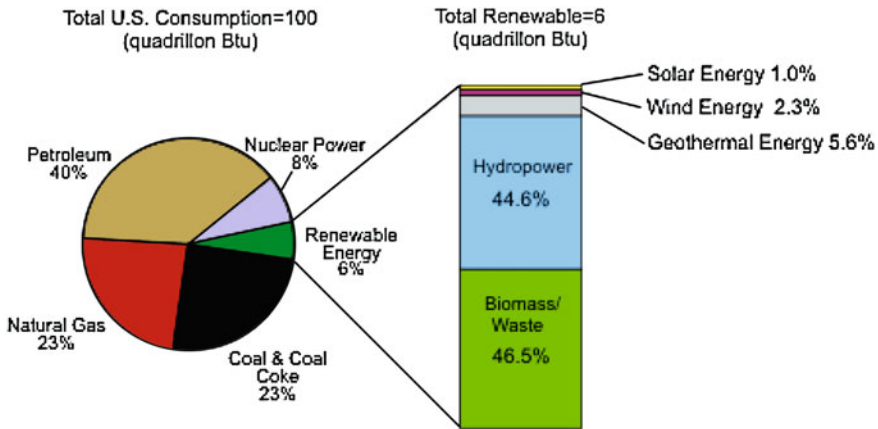


Fig. 14.1 Energy resources used in the United States [1]

According to the current energy resources used in United States as shown in Fig. 14.1, about 86% of the total energy is generated from fossil fuels, 8% is generated in nuclear plants, and remaining 6% comes from renewable sources (mainly hydro, biomass and wind power) [1]. Unfortunately, the world has limited amounts of fossil fuel and nuclear power resources. According to current estimates, natural uranium for nuclear power will last only about 50 years; oil will last no more than 100 years; gas, 150 years; and coal, 200 years [2]. Will the wheels of our civilization come to a screeching halt after the twenty-third century when fossil and nuclear fuels become totally exhausted?

Besides, our overdependence on fossil and nuclear fuels is causing environmental pollution and safety problems, which are now becoming dominant issues in our society. Rising pollution levels and worrying changing climate, arising in great part from energy-producing process, demand the reduction of ever-increasing environmentally damaging emissions. This impact of environmental pollution on global warming and resulting climate changes can have serious disastrous consequences in the long run [2].

At this juncture, we should be turning more and more to environmentally clean and safe renewable energy sources. Generating electricity, particularly by making use of renewable resources, allows the attainment of notable reductions of environmental pollution. Thereby, in addition to hydro-power used all over the world, the immense potentials of solar and wind energies assume great importance. Their promise is, however, subject to time-dependent process of nature. The systems needed to exploit them are still in their infancy. To establish themselves in a marketplace of high technical standards, a corresponding period for the development of these environmentally friendly technologies is particularly necessary [3].

The world has enormous resources of wind energy. This worldwide potential of wind power means that its contribution to electricity production can be of significant proportions. In some countries, the potential for wind energy



Fig. 14.2 World total wind power installed capacity [5]

production exceeds by far the local consumption of electricity. It has been estimated that tapping barely 10% of the wind energy available could supply all of the electricity needed in the world [3]. Good prospects and economically attractive expectations for the use of wind power are, however, linked to the incorporation of this weather-dependent power source into existing distribution networks.

14.1.2 The Scenarios for the Future on Wind Energy in the World

The worldwide market for wind energy has been growing faster than any other form of durable energy. Its installed power capacity in the world grew from only 4,800 MW in 1995 to 59,000 MW at the end of 2005 [4] that is, an increase of more than 1,200% in ten years. In the mean time, there are three scenarios worked out about how we can further expand wind energy and what benefits it will bring. Figure 14.2 shows the predicted world total installed capacity that is around 203,500 MW in 2010 [5]. Thus the total wind capacity will exceed 200,000 MW within the year 2010. Based on the accelerated development and further improved policies, world wind energy association (WWEA) is predicting that a global capacity of 1,900,000 MW will be possible by the year 2020 [5].

These predictions are impressive. In the expanding scenario we will be able to deliver 34% of our electricity from the wind energy by 2050 [4]. The cost price of wind energy can drop to 3 cents/kWh, the amount of jobs in the wind energy industries will result in a growth of 2.1 million, and the CO₂ emissions will decrease by 3,100 million tons. Wind energy is perhaps the most advanced among the “new” renewable energy technologies, but there is still much work to be done.

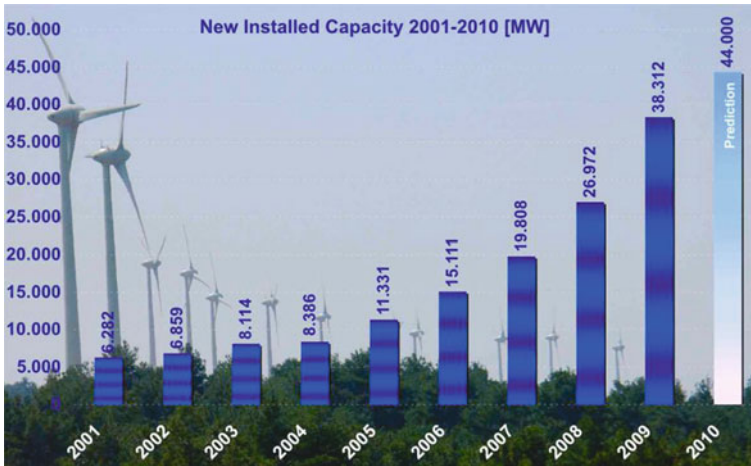


Fig. 14.3 World total new installed capacity [5]

This identifies the key tasks that must be undertaken in order to achieve a vision of over 2,000 GW of wind energy capacity by 2050 [6]. Figure 14.3 shows the world total new installed capacity up to 2010.

Therefore, a large number of wind turbine generators are going to be connected to the power system in the near future, percentage of wind farm output to the total power system capacity is expected to be fairly large. Wind farm composed of induction generators is considered in this work as it has some superior characteristics such as brushless and rugged construction, low cost, maintenance, and operational simplicity. But wind power is unsteady because wind speed is influenced by natural as well as meteorological situations. As the output power from wind farm fluctuating due to wind speed variations becomes large, fluctuations of the network frequency and voltage also become large. Though speed-governor system and pitch control system [7] can smooth the grid frequency and the wind farm output fluctuations up to a certain percentage, however, they are not sufficient to maintain network frequency to the desired level when the total wind power penetration into the grid is high. In this case, FACTS/ESS, i.e., FACTS with energy storage system (ESS), have recently emerged as more promising devices for power system applications [8].

Though every system has some advantages and at the same time some disadvantages, comparing among the ESS, superconducting magnetic energy storage systems (SMES) have received much attention among the researchers. The SMES is well known to be a system where energy is stored within a magnet that is capable of quickly releasing megawatt amounts of power. Since the successful commissioning test of the Bonneville Power Administration (BPA) 30 MJ unit [9], SMES systems have received much attention in power system applications. Thus SMES applications have been considered as new options to solve a variety of transmission, generation, and distribution system problems such as improvement

of voltage and angular stability, increasing power transfer capability of existing grids, damping subsynchronous oscillations, damping inter-area oscillations, load leveling, etc. [10–12]. The SMES system is combined with the voltage-source IGBT converter which is capable of effectively controlling and instantaneously injecting both active and reactive powers into the power system. This ability of injecting/absorbing real or reactive power substantially enhances the controllability and provides operation flexibility to a power system and is therefore a prospective option in building FACTS. Therefore, SMES seems to be a viable and alternate solution to resolve the frequency fluctuation caused by wind farm.

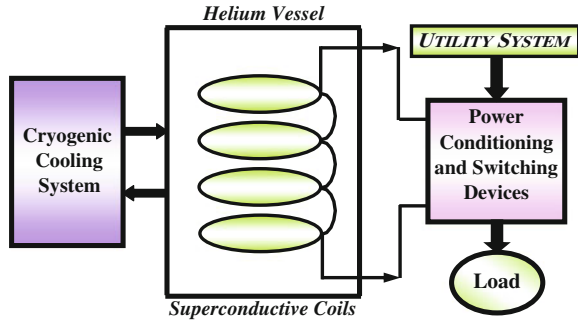
Therefore, in this chapter, a relationship between SMES power rating and the smoothing ability is analyzed considering multiple wind generator-based wind farm model. Because the output power of real wind farm is, in general, much smoother than that of a single wind generator [13], and hence the required SMES power rating can be smaller than 55%, which is the result in [14]. It is expected that large SMES capacity gives better smoothing performance. However, large capacity will definitely increase the system overall cost. Therefore, the optimum size determination of SMES is one of the key points from the viewpoint of cost-effectiveness. So, in this chapter, an evaluation method of SMES power rating is presented in light of wind farm real power fluctuation. Moreover, the minimum energy storage capacity of SMES unit to mitigate the frequency fluctuation is determined. Finally, performances of the proposed SMES with required power rating and minimum energy storage capacity to mitigate the frequency fluctuation are evaluated by using PSCAD/EMTDC [15].

14.2 Overview of SMES

A superconducting magnetic energy storage system is a DC current device for storing and instantaneously discharging large quantities of power. The DC current flowing through a superconducting wire in a large magnet creates the magnetic field. The large superconducting coil is contained in a cryostat or Dewar consisting of a vacuum vessel and a liquid vessel that cools the coil. A cryogenic system and the power conversion/conditioning system with control and protection functions [16] are also used to keep the temperature well below the critical temperature of the superconductor. During SMES operation, the magnet coils have to remain in the superconducting status. A refrigerator in the cryogenic system maintains the required temperature for proper superconducting operation. A bypass switch is used to reduce energy losses when the coil is on standby. And it also serves other purposes such as bypassing DC coil current if utility tie is lost, removing converter from service, or protecting the coil if cooling is lost [17].

Figure 14.4 shows a basic schematic of a SMES system [18]. Utility system feeds the power to the power conditioning and switching devices that provides energy to charge the coil, thus storing energy. When a voltage sag or momentary power outage occurs, the coil discharges through switching and conditioning devices, feeding conditioned power to the load. The cryogenic (refrigeration)

Fig. 14.4 Schematic diagram of the basic SMES system



system and helium vessel keep the conductor cold in order to maintain the coil in the superconducting state.

14.2.1 Advantages of SMES

There are several reasons for using superconducting magnetic energy storage instead of other energy storage methods. The most important advantages of SMES are that the time delay during charge and discharge is quite short. Power is available almost instantaneously and very high power output can be provided for a brief period of time. Other energy storage methods, such as pumped hydro or compressed air have a substantial time delay associated with the conversion of stored mechanical energy back into electricity. Thus if a customer's demand is immediate, SMES is a viable option. Another advantage is that the loss of power is less than other storage methods because the current encounters almost zero resistance. Additionally the main parts in a SMES are motionless, which results in high reliability. Also, SMES systems are environmentally friendly because superconductivity does not produce a chemical reaction. In addition, there are no toxins produced in the process.

The SMES is highly efficient at storing electricity (greater than 97% efficiency), and provide both real and reactive power. These systems have been in use for several years to improve industrial power quality and to provide a premium-quality service for individual customers vulnerable to voltage and power fluctuations. The SMES recharges within minutes and can repeat the charge/discharge sequence thousands of times without any degradation of the magnet [19]. Thus it can help to minimize the frequency deviations due to load variations [20]. However, the SMES is still an expensive device.

14.2.2 SMES for Load Frequency Control Application

A sudden application of a load results in an instantaneous mismatch between the demand and supply of electrical power because the generating plants are

unable to change the inputs to the prime movers instantaneously. The immediate energy requirement is met by the kinetic energy of the generator rotor and speed falls. So system frequency changes though it becomes normal after a short period due to Automatic Generation Control. Again, sudden load rejections give rise to similar problems. The instantaneous surplus generation created by removal of load is absorbed in the kinetic energy of the generator rotors and the frequency changes. The problem of minimizing the deviation of frequency from normal value under such circumstances is known as the load frequency control problem. To be effective in load frequency control application, the energy storage system should be fast acting i.e., the time lag in switching from receiving (charging) mode to delivering (discharging) mode should be very small. For damping the swing caused by small load perturbations, the storage units for LFC application need to have only a small quantity of stored energy, though its power rating has to be high, since the stored energy has to be delivered within a short span of time.

14.3 Model System Considered for Simulation Analyses

The model system shown in Fig. 14.5 has been used in the simulation analyses in this chapter [13]. The model system consists of a wind farm (WF), a hydropower generator, SG1, two thermal power generators, SG2 and SG3, a nuclear power generator, SG4, and a load. The wind farm consists of five wind power generators (squirrel-cage induction machines, IG n , $n = 1, 2, \dots, 5$). SG1 and SG3 are operated under Load Frequency Control (LFC) mode, SG2 is under Governor Free (GF) control mode, and SG4 is under Load Limit (LL) operation [21]. LFC is used, in general, to control frequency fluctuations with a long period more than a few minutes, and GF is used to control fluctuations with a short period less than a minute. LL is used to output constant power. A SMES is connected to the wind farm terminal bus.

Q_{WF} and Q_{Load} are capacitor banks. Q_{WF} is used at the terminal of WF to compensate the reactive power demand of the wind generators at steady state. The value of the capacitor (0.45 pu) is chosen so that power factor of the wind power station during the rated operation without SMES installed becomes unity [13, 22]. Q_{Load} is used at the terminal of load to compensate the voltage drop by the impedance of transmission lines. The initial conditions and parameters of IG's and SG's are shown in Tables 14.1 and 14.2, respectively.

14.4 Governor and AVR Systems

In this study, different types of AVR and Governor Systems are considered for synchronous generators as explained below:

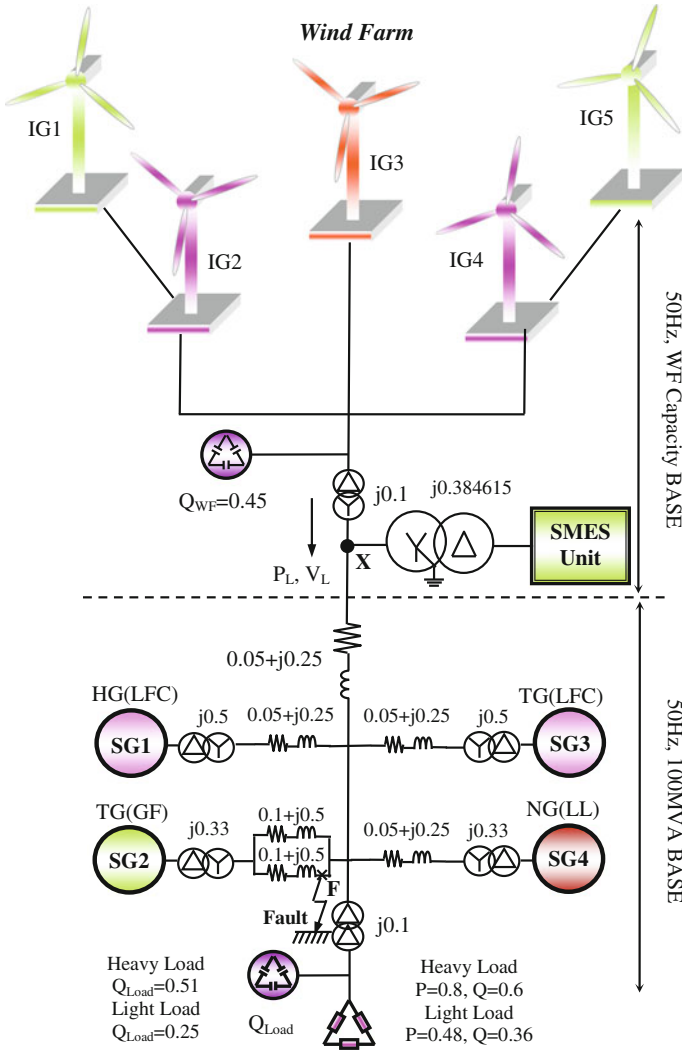


Fig. 14.5 Model system

Table 14.1 Initial conditions

	IG	SG1	SG2, SG3, SG4
P	0.1	1.00	1.00
V	1.00	1.05	1.05
Q	0.00	-	-
s(slipp)	-1.733%	-	-

Table 14.2 Parameters of generators [13]

Wind generator (induction generator)		squirrel-cage type (IGn, n = 1,2...5)		
MVA		2 (each)		
R ₁ (pu)		0.01		
X ₁ (pu)		0.10		
X _m (pu)		3.5		
R ₂₁ (pu)		0.035		
X ₂₁ (pu)		0.03		
R ₂₂ (pu)		0.014		
X ₂₂ (pu)		0.098		
2H s		1.5		
Synchronous generators				
	Salient pole type (SG1)	Cylindrical type		
		SG2	SG3	SG4
MVA	20	30	20	30
X _d (pu)	1.2		2.11	
X _q (pu)	0.7		2.02	
H s	2.5		2.32	

14.4.1 Governor for Hydro, Thermal, and Nuclear Generators

The IEEE “non-elastic water column without surge tank” turbine model and “PID control including pilot and servo dynamics” speed-governing system [23] shown in Fig. 14.6 is used for synchronous generator, SG1. The IEEE generic turbine model and approximate mechanical-hydraulic speed-governing system [24] shown in Fig. 14.7 is used for synchronous generators, SG2, SG3, and SG4. In the governor models shown in Figs. 14.6 and 14.7, the values of P_{ref} , initial output, P_0 , and turbine maximum output torque, $T_{m,max}$, are shown in Table 14.3, where, $\Delta\omega = \omega_{ref} - \omega$: the revolution speed deviation (pu), is set zero for SG1 and SG3 because these generators are operated under LFC to control frequency fluctuations with a relatively long period.

14.4.2 Automatic Voltage Regulator

Automatic Voltage Regulator (AVR) is used to keep the voltage of the synchronous generators constant. In the simulation analyses, IEEE alternator supplied rectifier excitation system (AC1A) [25] shown in Fig. 14.8 is used in the exciter model of all synchronous generators. Parameters of AVR model are shown in Table 14.4.

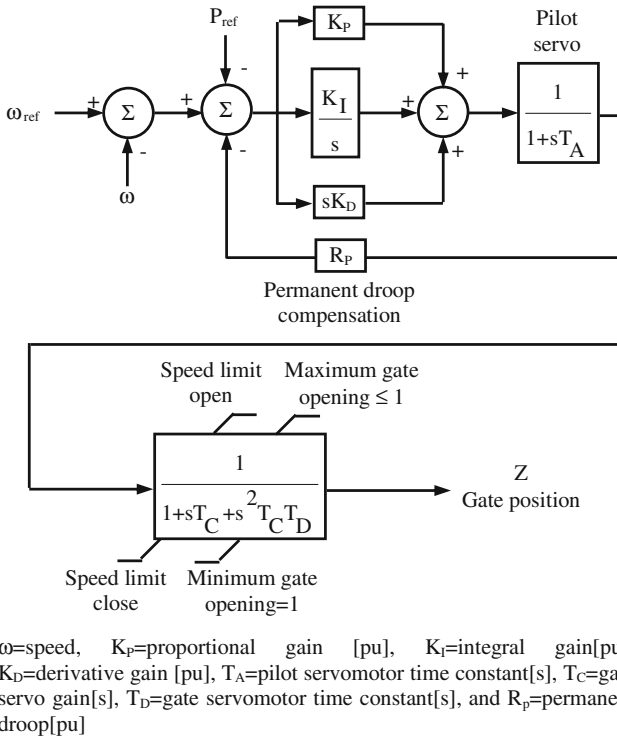


Fig. 14.6 Hydro governor [23]

14.4.3 Load Frequency Control Model

In the Load Frequency Control (LFC), the control output signal is sent to LFC power plant when the frequency deviation is detected in the power system. Then, governor command signal and thus the output of LFC power plant is changed according to LFC signal. The frequency deviation is input into Low Pass Filter (LPF) to remove fluctuations with short period because the LFC is used to control frequency fluctuations with a long period. The LFC model used in this study is shown in Fig. 14.9, where, T_c : the LFC period = 200 s; ω_c : the LFC frequency = $1/T_c = 0.005$ Hz; ζ : the damping ratio = 1.

14.5 Method of Calculating Power System Frequency

In this study, the index of the smoothing effect is used in power system frequency analysis. Power system frequency fluctuation is occurred due to unbalance between supply and load power in power system [26, 27]. Then, the frequency fluctuation

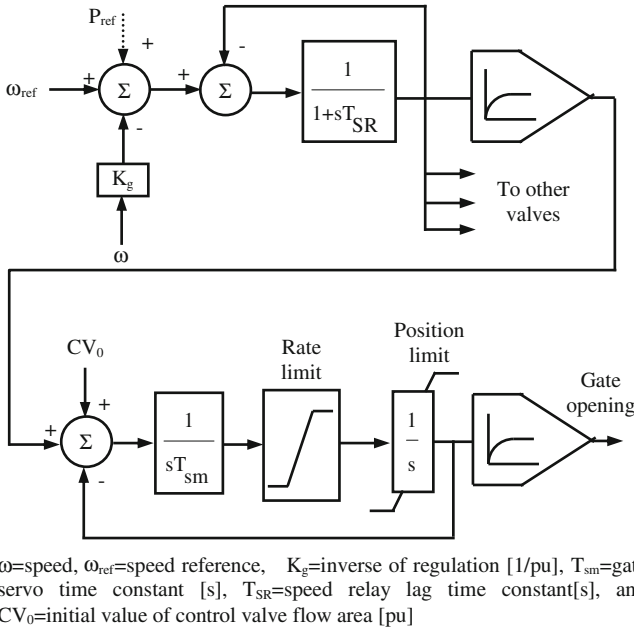


Fig. 14.7 Thermal and nuclear governors [24]

Table 14.3 Values of P_{ref} , P_0 and $T_{m,MAX}$ [13]

Load (MVA)	Frequency control SG1(Hydro)	P_{ref}	P_0	Frequency control SG2(Thermal)	P_0	$T_{m,max}$
100	LFC	LFC	0.75	GF	0.8	No limit governor
60		signal			0.4	completely free
	SG3(Thermal)			SG4(Nuclear)		
100	LFC	LFC signal	0.70	LL	0.90	0.80
60						

can be described by using two components, the rate of generator output variation, K_G (MW/Hz), and load variation, K_L (MW/Hz), respectively. They are representing the amount of power variation causing 1 (Hz) frequency fluctuation. When generator output variation, ΔG (MW), and load variation, ΔL (MW), are occurred, frequency fluctuation of the power system, ΔF (Hz), is expressed as follows:

$$\Delta F = \frac{\Delta G - \Delta L}{K_G + K_L} \tag{14.1}$$

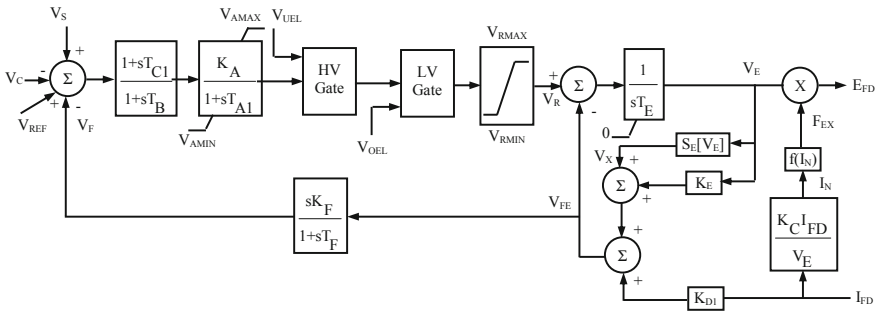
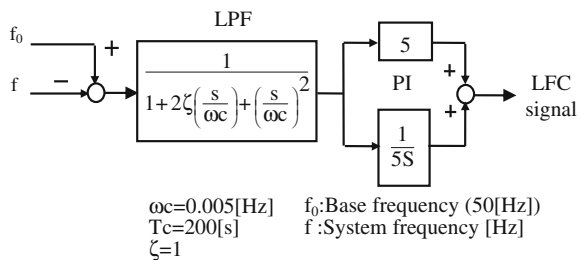


Fig. 14.8 AVR model system [25]

Table 14.4 Parameters of AVR

V_{REF} (pu)	1.05	K_C (pu)	0.20
K_A (pu)	400	K_D (pu)	0.38
T_A s	0.02	K_E (pu)	1.00
T_B s	0.00	T_E s	0.80
T_C s	0.00	K_F (pu)	0.03
V_{AMAX} (pu)	14.5	T_F s	1.00
V_{AMIN} (pu)	-14.5	$S_E V_{E1}$ (pu)	0.10
V_{RMAX} (pu)	6.03	$S_E V_{E2}$ (pu)	0.03
V_{RMIN} (pu)	-5.43	V_{E1} (pu)	4.18
V_{UEL}, V_{OEL}	Not applied	V_{E2} (pu)	3.14

Fig. 14.9 Load frequency control model

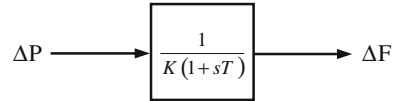


$$K = K_G + K_L \tag{14.2}$$

where, K is frequency characteristic constant.

In general, frequency characteristic is expressed as percentage K_G (expressed as $\%K_G$) for the total capacity of all generators and percentage K_L (expressed as $\%K_L$) for the total load. In general, it is known that $\%K_G$ and $\%K_L$ are almost constant and generally take a value of 8–15 and 2–6% (MW/Hz), respectively. However, K_L and K_G change greatly during a day because the number of parallel generators changes depending on the amount of load during a day. And, when power imbalance ΔP is occurred in power system, frequency fluctuation $\Delta P/K$ cannot occur immediately due to the governor characteristic and generator

Fig. 14.10 Frequency calculation model



inertia. Normally, ΔF converges to a new steady state value in 2–3 s. In general, when ΔP is changing slowly, relationship between ΔP and ΔF can be expressed as follows:

$$\frac{\Delta F}{\Delta P} = \frac{1}{K(1+sT)} \quad (14.3)$$

where, $\Delta P = \Delta G - \Delta L$.

Since changing load is not considered in this study, ΔL is “0”. Time constant, T (s), depending on the setting of generator governor and generator inertia, is generally 3–5 (s). In this study, power system capacity is assumed to be 100 (MW) and frequency characteristic K (MW/Hz) is selected to 8 (MW/Hz). This selection means that adjustability of the system frequency is weak, resulting a severe situation. Similarly, time constant T is selected to 3 s. In this study, frequency fluctuation in power system is evaluated by using Eq. 14.3. Therefore, frequency fluctuation, ΔF , is obtained as shown in Fig. 14.10.

14.5.1 Control System of SMES

The SMES system used is coupled (in Fig. 14.5) to the 66 kV line through a single step-down transformer (66/1.2 kV) with 0.384615 pu leakage reactance on the base value of 10 MVA, in this study. The proposed SMES [13] has the power rating and energy capacity of 2.6 MW and 312 MJ respectively, which will be explained later. Though SMES has virtually no resistance, the consideration of local LC resonance might be needed. However, as sub-synchronous resonance or shaft torsional oscillations are not the objective of this study, it is not considered here for simplicity. The control system of VSC used in this study is shown in Fig. 14.11. The SMES coil is charged or discharged by using the DC–DC chopper duty cycle (shown in Fig. 14.12). The parameters of PI controllers used in Figs. 14.11 and 14.13, which was determined by trial and error method are shown in Table 14.5.

14.5.2 Generation of Line Power Reference, P_{Lref}

IG line output power reference signal, P_{Lref} , is generated by the following way:

It is known from the results presented [28] that Low Pass Filter (LPF) method provides the best performance among the various reference generation methods

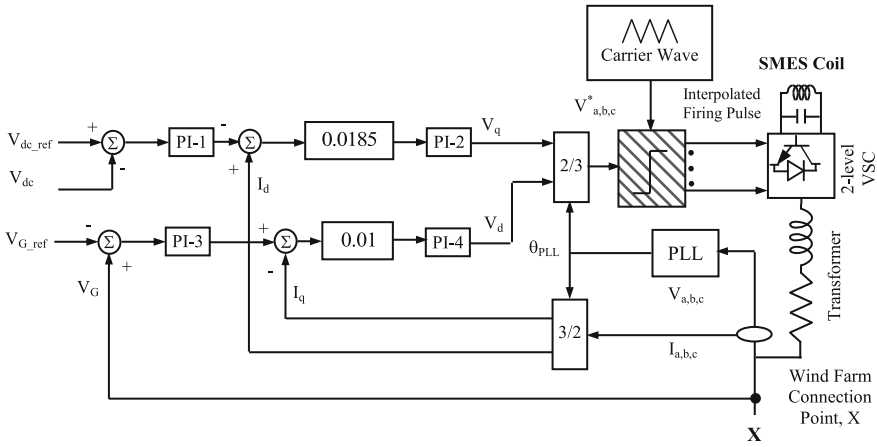


Fig. 14.11 Control system of the VSC [13]

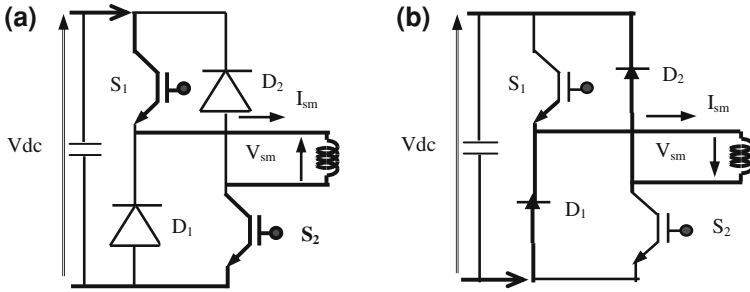
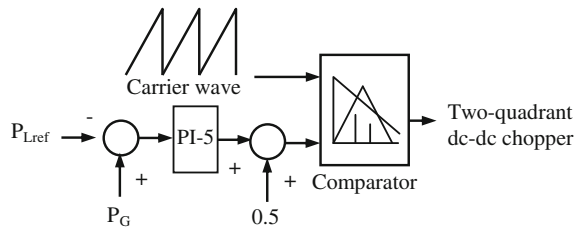


Fig. 14.12 The control concept of SMES charging and discharging mode

Fig. 14.13 Control system of two-quadrant DC-DC chopper



from the view points of the smoothing ability and energy storage capacity. Therefore, reference value of the transmission line power, P_{Lref} , is determined by using the LPF as shown in Fig. 14.14. The LPF suggests an increase or a decrease in the level of wind power output, which corresponds to charging or discharging of the stored energy.

Though it is very simple, it can be understood from Fig. 14.15 that reference value with enough smoothing effect can be obtained by using this type of LPF. Figure 14.15 shows an example how the time constant, T , affects the filtered wind

Table 14.5 Parameters of PI controllers

	PI-1	PI-2	PI-3	PI-4	PI-5
K_P	2.0	0.1	2.0	0.1	1.0
T_i	0.01	0.7	0.01	0.7	0.02

Fig. 14.14 Determination of reference line power

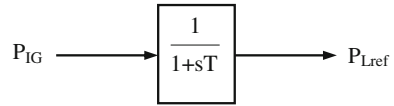
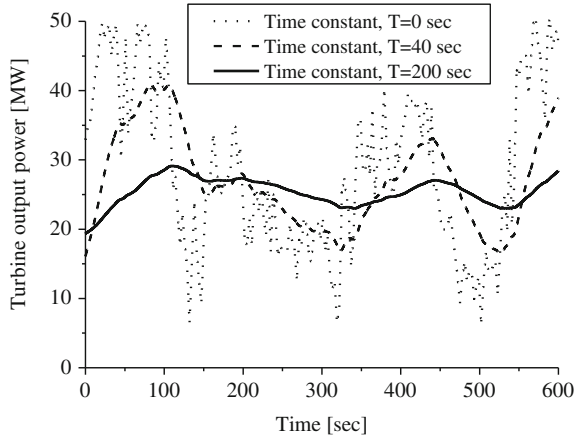


Fig. 14.15 Effect of time constant on the filtered wind power



power in practice. The values of T in the Fig. 14.15 correspond to energy storage system with different energy capacities. It is seen that the wind power fluctuation decreases as the LPF time constant increases. Therefore, if the transmission line power, P_{Lref} , is compensated according to the reference value, P_{Lref} , it is possible to decrease the system frequency fluctuation due to the wind generator output fluctuations.

The first-order passive low pass filter can be mathematically described as;

$$P_{IG} = P_{Lref} + T * P'_{Lref} \tag{14.4}$$

where T is the filtering time constant corresponding to energy storage capacity, P_{Lref} is the filter output function corresponding to the wind turbine output together with the storage unit, P'_{Lref} is the derivative of P_{Lref} and P_{IG} is the filter input function that corresponds to the wind turbine output without energy storage. When discrete data with a time step Δt are applied to a low pass filter and the derivative of P_{Lref} is expanded into a discrete form, Eq. 14.4 can be written for step k as

$$T \frac{P'_{Lref,k} - P'_{Lref,k-1}}{\Delta t} + P'_{Lref,k} = P_{IG,k} \tag{14.5}$$

Solving for $P_{\text{Lref}, k}$ gives

$$P_{\text{Lref}, k} = \frac{T}{T + \Delta t} P_{\text{Lref}, k-1} + \frac{\Delta t}{T + \Delta t} P_{\text{IG}, k} \quad (14.6)$$

Defining a constant $\beta = \frac{T}{T + \Delta t}$, Eq. (14.6) can be rewritten as

$$P_{\text{Lref}, k} = \beta P_{\text{Lref}, k-1} + (1 - \beta) P_{\text{IG}, k} \quad (14.7)$$

Now Eq. (14.7) has the form of an exponentially weighted moving average (EWMA) filter [29]. The subscript k corresponds to time, i.e. $t_k = t_0 + k\Delta t$, where Δt is the time step and t_0 is the starting point of the analysis.

With an EWMA filter the response of the energy storage system is

$$P_{\text{st}, k} = P_{\text{IG}, k} - P_{\text{Lref}, k} \quad (14.8)$$

where $P_{\text{st}, k}$ is the power absorbed by the storage unit. Thus, the level of the stored energy in the system is in discrete form as

$$E_k = \sum_{m=1}^k P_{\text{st}, m} \Delta t \quad (14.9)$$

The energy storage capacity used for damping the fluctuations is then defined as

$$E_{\text{storage}} = \max E_k - \min E_k, \text{ for } k = 1 \dots n \quad (14.10)$$

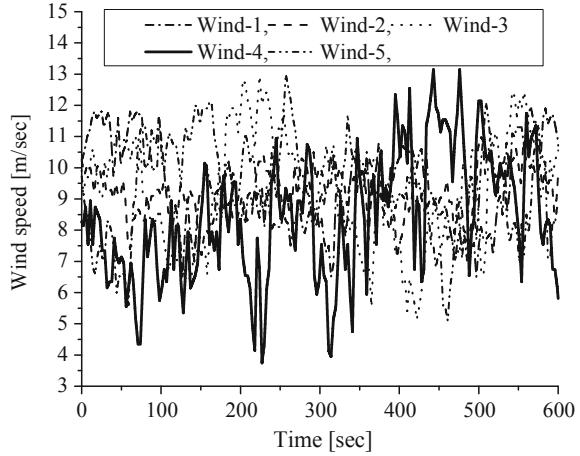
where n is the total number of time points in the data sample.

14.6 Analysis of SMES Power Rating

Since a large number of wind turbine generators are going to be connected to power system in the near future, percentage of wind farm output to the total power system capacity is expected to be fairly large, and thus 10% (10 MW) wind power penetration is assumed in this study [13]. In this section, the relationship between SMES power rating and the smoothing ability is investigated by evaluating a wind farm output, P_{WF} , and reference value of transmission line power, P_{Lref} .

An interesting study has been performed in [14], where the SMES power rating to minimize the frequency fluctuation is determined by using single wind generator model which represents the aggregated wind farm. It is reported therein that SMES power rating of 55% of that of the wind farm is required to mitigate the frequency fluctuation of the grid. However, aggregated model of wind farm is not sufficient for the analysis because the output power of real wind farm is, in general, much more smooth than that of a single wind generator, and hence the required SMES power rating can be smaller than 55%, which is the result in [14]. Therefore, in this chapter the multiple wind generator-based wind farm model is used instead of a

Fig. 14.16 Responses of wind speed data [Case-I & II]



single wind generator to determine the power rating of SMES unit more precisely. Then, the minimum energy storage capacity of SMES unit is also determined.

In this study, a wind farm of five wind generators with different wind speed patterns with relatively large fluctuations shown in Fig. 14.16 and Table 14.6, respectively is used in the analysis. In order to estimate a required power rating of the SMES, smoothing effect of the wind farm output is investigated by using P_{Lref} which is obtained through EWMA filter with considering several time constants. The effect of energy storage capacity on grid frequency fluctuations is also discussed.

SMES output is obtained as $P_{st,k}$ of Eq. (14.8) in this analysis, and then a standard deviation of the SMES output, σ , is calculated. In addition, smoothing effect is evaluated by using frequency fluctuation, Δf . Power rating of the SMES required for smoothing wind farm output and EWMA time constant suitable for the reference value with enough smoothing effect are investigated by using σ and Δf in this analysis. Table 14.7 shows σ and maximum Δf for each EWMA time constant.

Figure 14.17 shows the maximum frequency fluctuation with respect to EWMA time constant. Table 14.7 shows that the frequency fluctuation decreases as EWMA time constant increases. Therefore, if the transmission line power is compensated according to the reference value, P_{Lref} , it is possible to decrease the system frequency fluctuation due to the wind farm output fluctuations. It is clear from Fig. 14.17 that the maximum frequency fluctuation is very small when EWMA time constant is over about 120 s.

Figure 14.18 shows standard deviation, σ , of the SMES output with respect to EWMA time constant. σ increases as EWMA time constant increases. However, as can be seen from the figure, the function of σ is not monotonous and it saturates where EWMA time constant is over about 120 s. Therefore, almost no improvement can be obtained by adopting longer EWMA time constant than 120 s and corresponding power rating of SMES. From these results, the reference value of

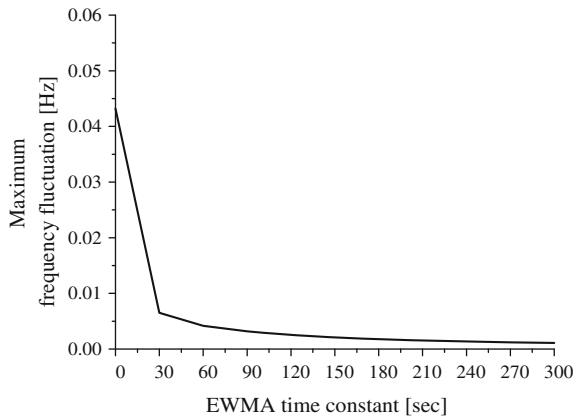
Table 14.6 Wind speed condition of each generator [13]

Wind data's name	Average wind speed (m/s)	Standard deviation of wind speed (m/s)
Wind-1	Medium 9.44	Medium 1.39778
Wind-2	Medium 9.20	Medium 1.28063
Wind-3	Medium 9.30	Large 1.79351
Wind-4	Medium 8.27	Large 1.98949
Wind-5	Medium 9.42	Medium 1.55302

Table 14.7 Standard deviation of SMES output and maximum frequency fluctuation [13]

EWMA time constant (s)	10 MW wind farm	
	Δf (Hz)	σ (MW)
0	0.04320	0.00000
30	0.00651	0.65140
60	0.00419	0.75406
90	0.00317	0.84607
120	0.00253	0.86469
150	0.00209	0.86984
180	0.00178	0.87161
210	0.00154	0.87786
240	0.00135	0.88310
270	0.00120	0.88631
300	0.00108	0.88813

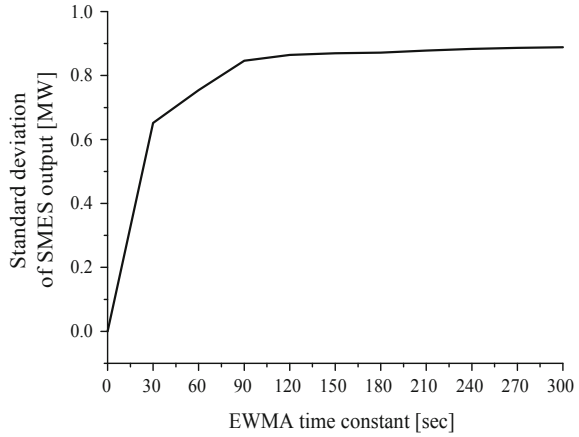
Fig. 14.17 Response of frequency fluctuation



transmission line power corresponding to σ for 120 s of EWMA time constant can be considered sufficient for the smoothing control. Consequently it can be said that, if 120 s time constant is adopted in EWMA filter, the suitable reference value with enough smoothing effect can be obtained.

If the power rating of SMES is determined based on the value of 3σ , approximately 99.7% of necessary smoothing effect can be achieved according to the characteristics of standard deviation as shown in Fig. 14.19. Therefore, if the

Fig. 14.18 Response of standard deviation of SMES output



SMES power rating is determined to 2.6 (MW) ($3\sigma = 3 \times 0.86469 = 2.59407 \approx 2.6$), it can be considered to be sufficient for the smoothing control of 10 (MW) wind farm. In the following simulation analyses, the SMES with 2.6 (MW) power rating is used with considering the same wind speed patterns and the effect of energy storage capacity of SMES on grid frequency fluctuations is investigated. Finally, the minimum energy storage capacity of SMES unit is determined.

14.7 Simulation Results

Simulation analyses are carried out to investigate the performance of the proposed controlled SMES [13]. The power capacity of SMES is 26% of that of the wind farm and several values are considered for its energy capacity in the analyses to determine its optimal value. The analyses have been performed by using PSCAD/EMTDC. Two cases are considered as given below:

Case-I, light load: The load is 60 MVA and all generators are in service except SG3. This case is more severe than Case-II from a viewpoint of system frequency control.

Case-II, heavy load: The load is 100 MVA and all generators are in service.

The real wind speed data shown in Fig. 14.16 is applied to each wind generator. The time step and simulation time have been chosen as 0.00001 and 600 s, respectively. Three energy capacities are considered for SMES in the analyses, which are 60, 90, and 120 s of the power rating (for example, the capacity is $2.6 \text{ MW} \times 120 \text{ s} = 312 \text{ MJ}$ in the case of 120 s). Figure 14.20 shows the responses of SMES energy storage level for the wind speed data of Fig. 14.16. Figures 14.21 and 14.22 show the responses of the line power in the cases of

Fig. 14.19 Characteristics of standard deviation

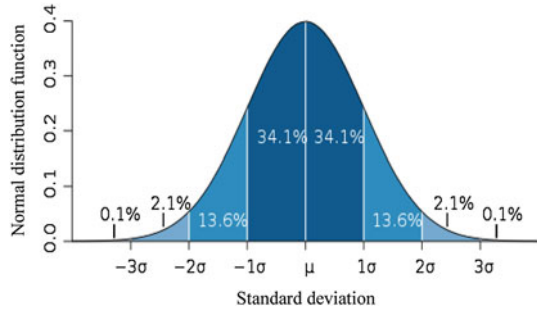
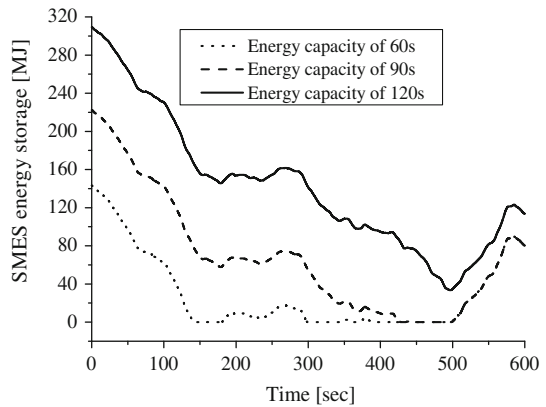


Fig. 14.20 Responses of SMES energy storage level [Case-I & II]



SMES energy capacity of 60 and 90 s for Case-I. It is clearly seen from the figures that the wind farm output cannot be smoothed in these cases. Also the system frequency cannot be maintained within the acceptable range as seen from Fig. 14.23. Similarly, it is seen from Fig. 14.24 that the system frequency cannot be maintained within the acceptable range also for Case-II.

As a result, 120 s can be expected to be optimal for the energy capacity of SMES unit, and detailed simulation analyses are performed using this value as shown in the following:

Figure 14.25 shows the wind farm output, which is fluctuating due to the wind speed variations in the case without SMES. But when SMES of 120 s energy capacity is installed, the line power can be smoothed effectively. Figures 14.26 and 14.27 show the output of hydro-power generator (SG1) and thermal power generator (SG3) respectively in the cases with and without SMES considered which are comparatively smooth. This is because these generators are operated under LFC to control the electric power fluctuations with long period. As SMES provides proper compensation for randomly varying wind farm output, SG1 and SG3 are generating comparatively less power to supply to the load as shown in Figs. 14.26 and 14.27 respectively for both cases. Figure 14.28 shows the thermal power generator (SG2) output. The response without SMES is fluctuating so much

Fig. 14.21 Responses of wind farm line real power [Case-I]

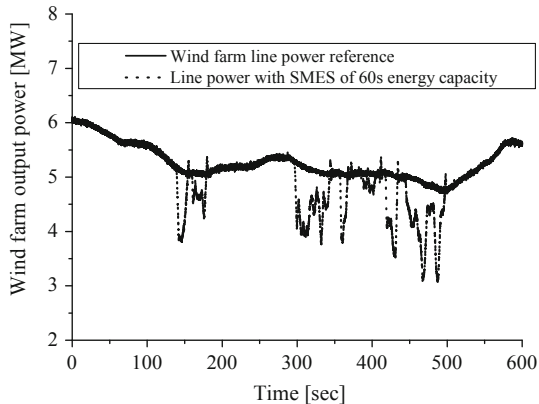


Fig. 14.22 Responses of wind farm line real power [Case-I]

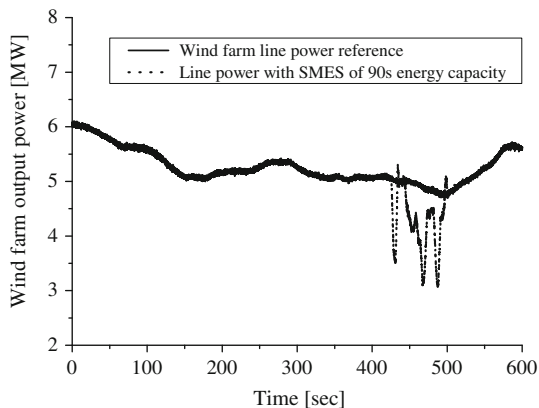


Fig. 14.23 Responses of power system line frequency [Case-I]

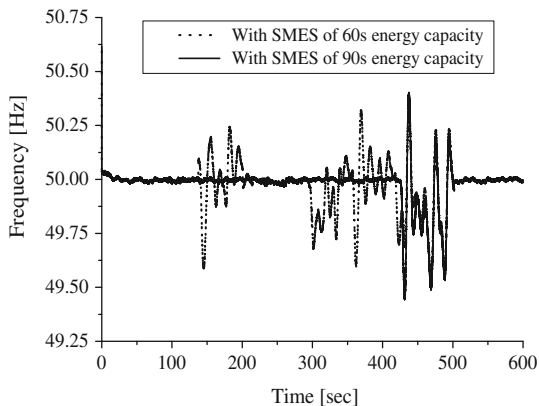


Fig. 14.24 Responses of power system frequency [Case-II]

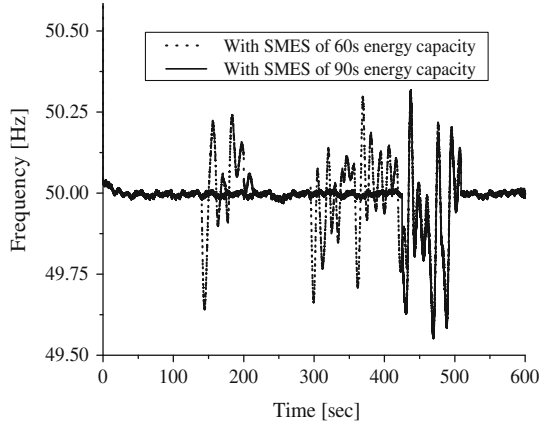
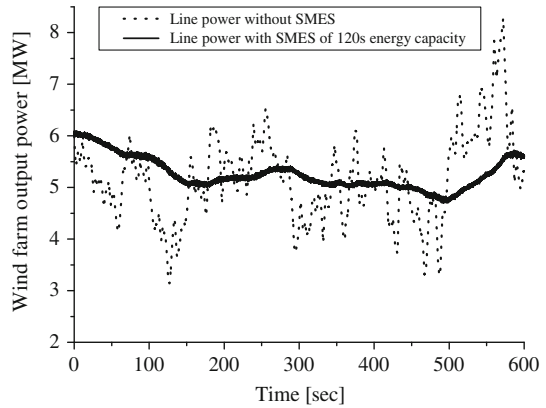


Fig. 14.25 Responses of wind farm line real power [Case-I & II]



because this generator is operated under GF to control the electric power fluctuations with short period.

However, in the case with considering SMES, the response does not vary so much because the grid power from the wind farm is smooth as shown in Fig. 14.25. Figure 14.29 shows the nuclear power generator (SG4) output, where the responses are maintained almost constant because this generator is operated under LL operation for both cases. Figure 14.30 shows the response of the SMES real power. It is seen that under the condition of randomly varying wind speed the SMES provide proper compensation of real power according to the variation of line power to maintain the grid frequency. Figures 14.31 and 14.32 show the power system frequency with and without using SMES for Case-I and II, respectively. When the power capacity of the wind farm is relatively large compared with that of the power system, the power system frequency cannot be maintained well by the frequency control of synchronous generators. But it can be maintained well to the rated value by the proposed controlled SMES. Moreover, frequency fluctuation without SMES is bigger in Case-I (light load) than in Case-II

Fig. 14.26 Responses of hydro-power generator (SG1) outputs

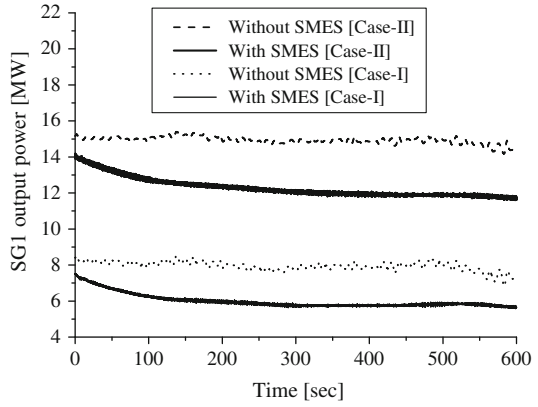


Fig. 14.27 Responses of thermal power generator (SG3) outputs

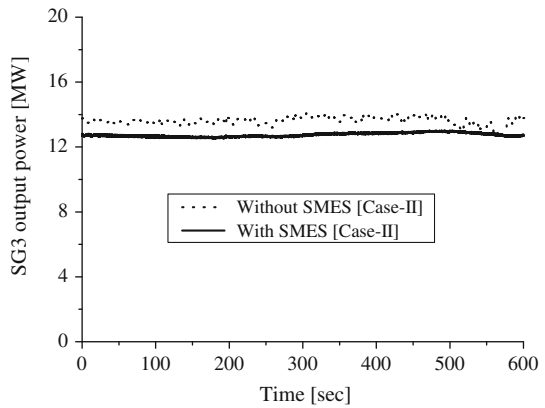


Fig. 14.28 Responses of thermal power generator (SG2) outputs

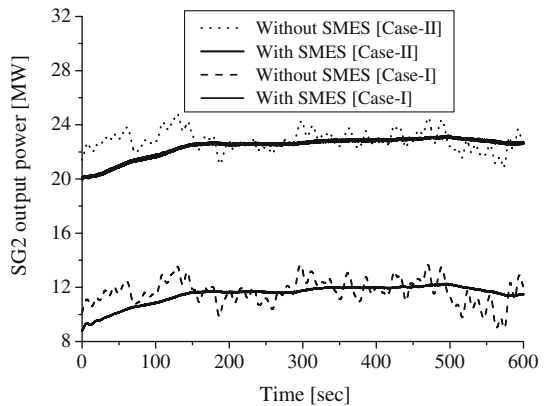


Fig. 14.29 Responses of nuclear power generator (SG4) outputs

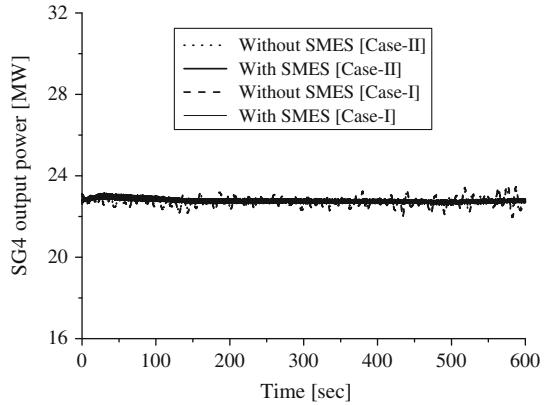
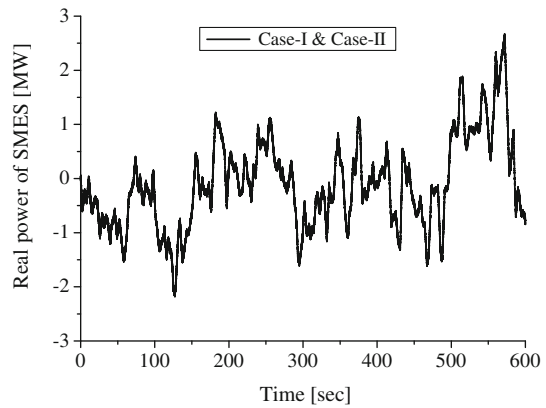


Fig. 14.30 Response SMES real power [Case-I & II]



(heavy load) as shown in Figs. 14.31 and 14.32, respectively. This is because one of the LFC synchronous generators must be stopped during the light load. Table 14.8 shows the maximum frequency fluctuation in the cases without and with SMES unit for each energy storage capacity.

Wind farm grid voltage can also be maintained constant by using the proposed SMES system as seen from Fig. 14.33. This fact indicates that the proposed controlled SMES can also decrease the voltage fluctuations.

From the simulation results shown in Figs. 14.25, 14.26, 14.27, 14.28, 14.29, 14.29, 14.30, 14.31, 14.32 and 14.33 and Table 14.8, it is seen that suitable reference value for the wind farm output can be obtained and then sufficient smoothing effect can be achieved by using the proposed SMES system.

Finally, it is concluded that the line power reference generation scheme using EWMA is very effective and the proposed SMES system can provide sufficient smoothing effect on the wind farm output as well as the grid system frequency fluctuations.

Fig. 14.31 Responses of power system frequency [Case-I]

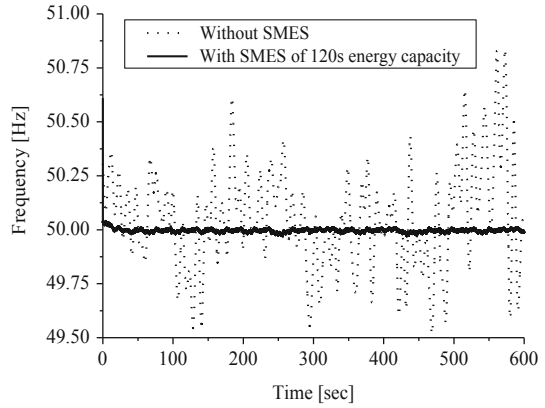


Fig. 14.32 Responses of power system frequency [Case-II]

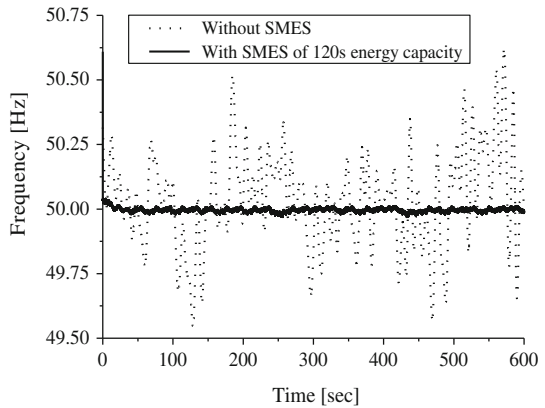
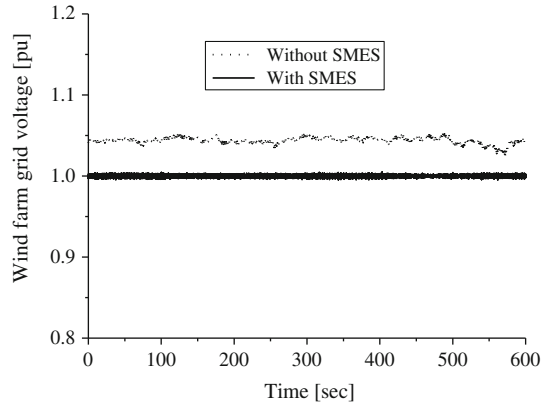


Table 14.8 Maximum frequency fluctuation in each condition [13]

Load (MVA)	Wind farm capacity 10 MVA		
	Δf (Hz) without SMES	SMES energy capacity (s)	Δf (Hz) with SMES
60	0.83671	60	0.53416
		90	0.55683
		120	0.02408
100	0.62123	60	0.43312
		90	0.44866
		120	0.02275

Fig. 14.33 Responses of wind farm terminal voltages



14.8 Conclusions

This chapter presents a sinusoidal PWM voltage-source converter and two-quadrant DC–DC chopper-controlled SMES for smoothing output power fluctuations of wind farm in order to maintain the grid frequency deviation within an acceptable range. The method of determining the power rating of the SMES is also presented. An EWMA filter is used to generate the reference value for the wind farm output. The effect of the smoothing control is evaluated using a power system model installed with the SMES unit, which has a power rating of 26% of the wind farm capacity and an energy capacity of 2 min multiplied by the power rating. These values of the SMES power rating and energy capacity are found to be optimum for the wind speed pattern obtained in Hokkaido, Japan, in which the speed fluctuation is very large compared with that in Europe. The simulation analyses show that, using the proposed SMES system, the wind farm output fluctuations can be decreased, and hence the frequency of the grid system, can be maintained within an acceptable range. Therefore, the integration of the proposed SMES system into a wind farm can be an effective means of mitigating the frequency fluctuations of the grid system.

References

1. http://en.wikipedia.org/wiki/Energy_in_the_United_States
2. Simoes MG, Farret FA (2004) Renewable energy system, design and analysis with induction generators. CRC Press, Washington, D.C
3. Heier S (1998) Grid integration of wind energy conversion systems. Wiley, Chicester, UK
4. <http://www.olino.org/us/articles/category/wind-energy>
5. World Wind Energy Association; Available online in <http://www.wwindea.org/home/index.php>
6. <http://www.olino.org/us/articles/2009/12/03/technology-roadmap-wind-energy-iea>

7. Yamazaki T, Takahashi R, Murata T, Tamura J, Fukushima T, Sasano E, Shinya K, Matsumoto T (2009) Smoothing control of wind generator output fluctuations by new pitch controller. *IEEJ Trans Power Energy* 129(7):880–888
8. Zhang L, Shen C, Crow ML, Dong L, Pekarek S, Atcitty S (2005) Performance indices for the dynamic performance of FACTS and FACTS with energy storage. *Electr Power Compo Syst* 33(3):299–314
9. Boenig HJ, Hauer JF (1985) Commissioning tests of the Bonneville power administration 30 MJ superconducting magnetic energy storage unit. *IEEE Trans Power Apparatus Syst* 104(2):302–309 PAS
10. Mitani Y, Tsuji K, Murakami Y (1988) Application of superconducting magnetic energy storage to improve power system dynamic performance. *IEEE Trans Power Syst* 3: 1418–1425
11. Banerjee S, Chatterjee JK, Tripathy SC (1990) Application of magnetic energy storage unit as load frequency stabilizer. *IEEE Trans Energ Convers* 5:46–51
12. Wu CJ, Lee YS (1991) Application of superconducting magnetic energy storage unit to improve the damping of synchronous generator. *IEEE Trans Energ Convers* 6(4):573–578
13. Sheikh MRI, Muyeen SM, Takahashi R, Murata T, Tamura J (2010) Smoothing Control of Wind Generator Output Fluctuations by PWM Voltage Source Converter and Chopper Controlled SMES. *European Transactions on Electrical Power*, 21(1):1–18, Published online in Wiley InterScience (<http://www.interscience.wiley.com>). DOI: 10.1002/etep.469
14. Asao T, Takahashi R, Murata T, Tamura J, Kubo M, Kuwayama A, Matsumoto T (2007) Smoothing control of wind power generator output by superconducting magnetic energy storage system. *ICEMS*, Seoul, Korea, pp 302–307
15. PSCAD/EMTDC Manual (1994) Manitoba HVDC Research Center
16. IEEE task force on benchmark models for digital simulation of FACTS, custom–power controllers, T&D committee, (2006) Detailed modeling of superconducting magnetic energy storage (SMES) system. *IEEE Trans Power Delivery* 21(2):699–710
17. Ali MH, Murata T, Tamura J (2008) Transient stability enhancement by fuzzy logic-controlled SMES considering coordination with optimal reclosing of circuit breakers. *IEEE Trans Power Syst* 23(2):631–640
18. http://www.doc.ic.ac.uk/~matti/ise2grp/energystorage_report/node8.html
19. http://en.wikipedia.org/wiki/Superconducting_magnetic_energy_storage
20. Demiroren A, Yesil E (2004) Automatic generation control with fuzzy logic controllers in the power system including SMES units. *Int J Electr Power Energy Syst* 26:291–305
21. IEE of Japan, Standard Models of Electrical Power System. Technical Reports, 754:40–43
22. Sheikh MRI, Muyeen SM, Takahashi R, Murata T, Tamura J (2008) Wind generator stabilization by PWM voltage source converter and chopper controlled SMES. *J Int Rev Autom Control (I.RE.A.CO)* 1(3):311–320
23. Working group on prime mover, energy supply models for system dynamic performance studies (1992) Hydraulic turbine and turbine control models for system dynamic studies. *IEEE Trans Power Syst* 7(1):167–179
24. Working group on prime mover, energy supply models for system dynamic performance studies (1991) Dynamic models for fossil fuelled steam units on power system studies. *IEEE Trans Power Syst* 6(2):753–761
25. IEEE recommended practice for excitation system models for power system stability studies, IEEE Std. 421.5-1992
26. Koike T (1979) Electric power transmission and distribution. Youkendo. Co. Ltd, Tokyo, Japan
27. Sekine Y (1966) Power system engineering. Denkishoin. Co. Ltd, Tokyo
28. Sheikh MRI (2010) Stabilization of a grid-connected wind farm by using SMES. Ph.D. Thesis
29. Paatero JV, Lund PD (2005) Effect of energy storage on variations in wind power. *Wind Energ* 8:421–441